Electronic Supplementary Material (ESI) for Journal of Materials Chemistry C.

Impact of carrier diffusion on internal quantum efficiency of InGaN quantum well structures

Supporting Information: 8 pages, 7 figures, 1 table

Kazimieras Nomeika, Žydrūnas Podlipskas, Mariamija Nikitina, Saulius Nargelas, Gintautas Tamulaitis, and Ramūnas Aleksiejūnas

Vilnius University, Institute of Photonics and Nanotechnology, Saulėtekio Ave. 3, LT-10257, Vilnius, Lithuania

(Dated: 9 December 2021)

Table S1. The parameters of QW structures used in the study. Colours roughly match the visible emission.

Sample	QW width	QW periods	Barrier width	QW In content	Cap thickness	Buffer layer	TIPL peak	TIPL FWHM
							at peak IQE	
	nm	count	nm	%	nm	type	eV	
S1	2	6	3	23	(+)25	nGaN+SC	3	0.14
S2	2	6	3	20	(+)100	nGaN+SC	2.96	0.13
S3	2	6	12	20	(+)100	nGaN+SC	2.93	0.14
S4	3	6	3	17	(+)50	nGaN+SC	2.93	0.13
S5	3	5		30	(+)120	nGaN	2.36	0.12
S6	3	5		26	(+)120	nGaN	2.5	0.14
S7	4	1		22	(+)120	nGaN	2.76	0.14
S8	3	5			(+)120	nGaN	2.79	0.11
S9	3.5	5	6	8	30	uGaN+SL	2.68	0.16
S10	3.5	5	6	8	30	uGaN	2.81	0.20
S11	3.5	5	6	8	23	uGaN	2.79	0.12
S12	3.5	5	6	8	23	uGaN	2.8	0.14
S13	3.5	5	6	8	(+)300	nGaN+SL	2.8	0.16
S14	4.7	5	18	5.1	18	nGaN	2.98	0.18
S15	4.2	5	18	8.4	18	nGaN	2.77	0.22
S16	6	5	18	11.3	18	nGaN	2.82	0.17
S17	5.8	5	18	13.2	18	nGaN	2.74	0.17
S18	5	5	18	23	18	nGaN	2.63	0.20
S19	3.5	4	4.5	15	(+)88	nGaN+SC	2.87	0.12
S20	3.5	6	4.5	15	(+)88	nGaN+SC	2.81	0.17
S21	2.6	10	7.1	18.9	7	uGaN	2.79	0.10
S22	2.6	10	7.1	17.4	7	uGaN	2.78	0.11
S23	2.6	10	7.1	18	7	uGaN	2.74	0.12
S24	2.6	10	7.1	18	7	uGaN	2.74	0.13
S25	3.1	5	7.1	12	8	uGaN+SL	2.74	0.15
S26	3.7	5	6.6	12	8	uGaN+SL	2.66	0.20
S27	3.1	5	7.8	12	8	uGaN+SL	2.56	0.27
S28	3.9	5	7.8	12	8	uGaN+SL	2.35	0.29
S29	4.2	5	8.7	12	8	uGaN+SL	2.31	0.27
S30	4.5	5	7.7	12	8	uGaN+SL	2.25	0.29
S31	4.5	5		12	8	uGaN+SL	2.21	0.39
S32	4.8	5	9	12	8	uGaN+SL	2.13	0.44
S33	4.1	5	6.7	10.5	28	uGaN+SL	2.62	0.16
S34	4.1	5	6.7	10	28	uGaN+SL	2.6	0.17
S35	3.8	5	7.2	9.5	28	uGaN+SL	2.66	0.15
S36	4.1	5	6.7	10	28.5	uGaN+SL	2.65	0.17
S37	4.1	5	6.8	9	28.5	uGaN+SL	2.64	0.15
S38	3.8	5	6.6	10.5	28	uGaN+SL	2.59	0.14
S39	3.8	5	6.6	10	28	uGaN+SL	2.63	0.13
S40	3.8	5	6.6	10	28	uGaN+SL	2.65	0.13
S41	1	8	12	25	(+)38	nGaN	2.9	0.14
S42	1	8	12	25	(+)30	nGaN	2.86	0.14
S43	2	8	12	25	(+)38	nGaN	2.51	0.14
S44	2.7	8	12	25	(+)38	nGaN	2.26	0.13
S45	4	8	12	25	(+)38	nGaN	2.69*	0.15*
S46	8.2	3	8.8	13.3	(+)143	nGaN	2.93	0.27
S47	8.2	3	8.8	9.2	(+)143	nGaN	3.04	0.10
S48	6.8	3	8.8	13.1	(+)143	nGaN	2.98	0.15
S49	7.8	3	8.8	10.4	(+)143	nGaN	2.98	0.23
S50	8.2	3	14.8	13.2	(+)143	nGaN	2.93	0.21
S51	4.5	3	14.8	13.5	(+)143	nGaN	2.83	0.29
S52	4.5	3	14.8	13.5	(+)143	nGaN	2.87	0.25
S53	3	10	10	10	8	uGaN	2.96	0.11
S54	3	10	12	9	12	uGaN	3.12	0.10
S55	3	10	12	12	12	uGaN	2.94	0.10
S56	3	10	12	17	12	uGaN	2.62	0.12
S57	3	10	12	20	12	uGaN	2.39	0.14

(+) - p-doped cap
nGaN - n-doped GaN
uGaN - undoped GaN
SC - staircase interlayer
SL - superlattice
* - most intense peak

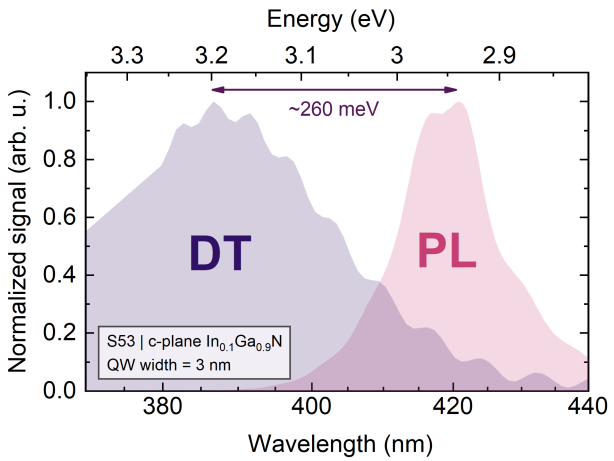

Figure S1. An example of a large Stokes shift between the photoluminescence and differential absorption spectra in a c-plane InGaN MQW structure.

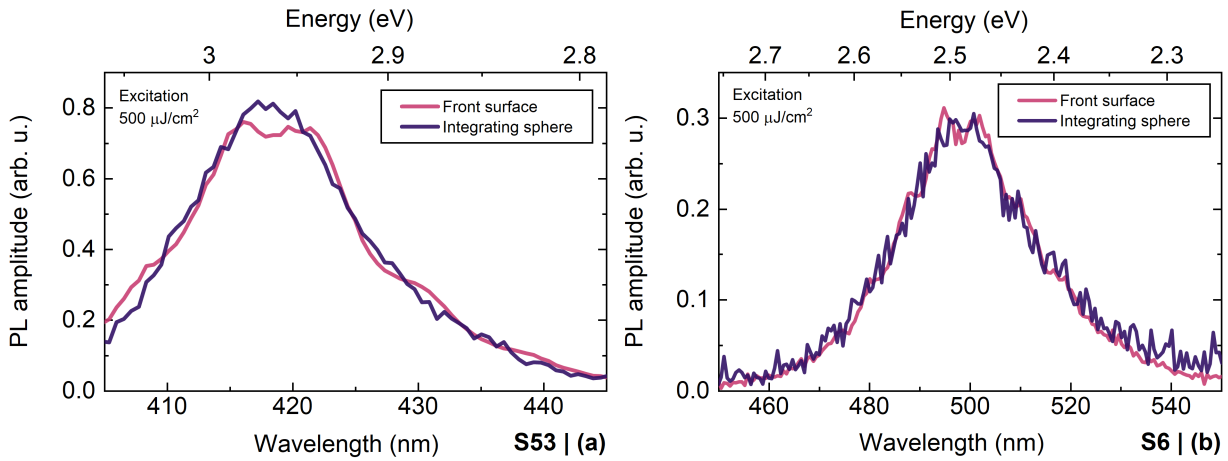

Figure S2. PL spectra recorded in the integrating sphere (violet line) and outside of it by collecting PL from the front surface (magenta line) in the samples S53 (a) and S6 (b).

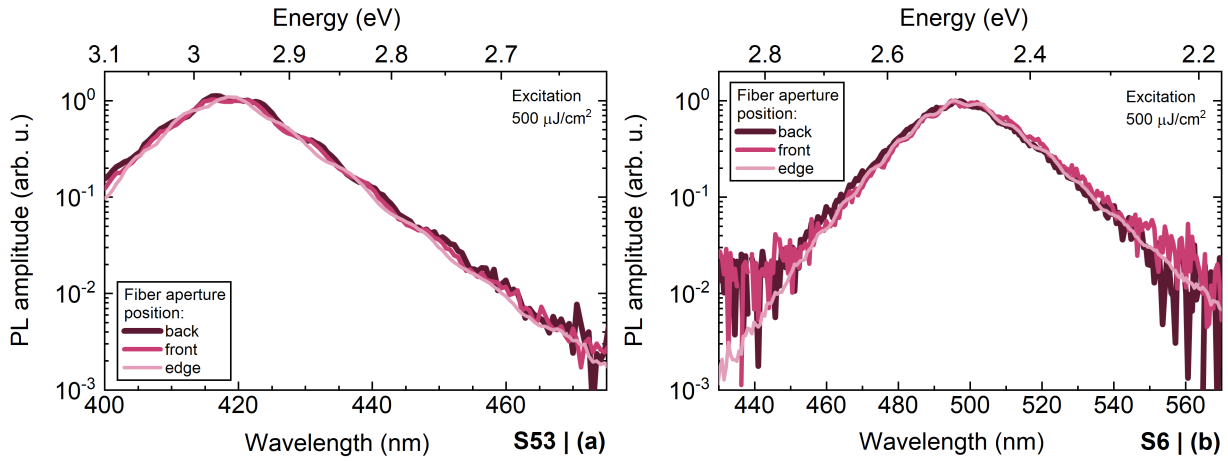

Figure S3. Normalized PL spectra collected from the front surface (magenta line), the back surface (violet line), and the sample edge (light magenta line) in S53 (a) and S6 (b).

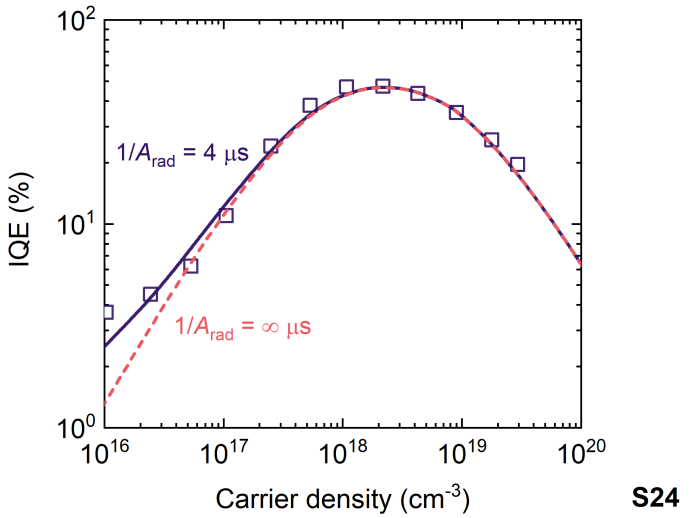

Figure S4. The illustration for the necessity of the A_{rad} coefficient in the ABC model. The violet curve illustrates the $\mathrm{IQE}_{\mathrm{calc}}(N)$ calculated using equation 3 in the main text with $1/A_{\mathrm{rad}} = 4$ μs, while the magenta dashed line shows the case for $A_{\mathrm{rad}} = 0$.

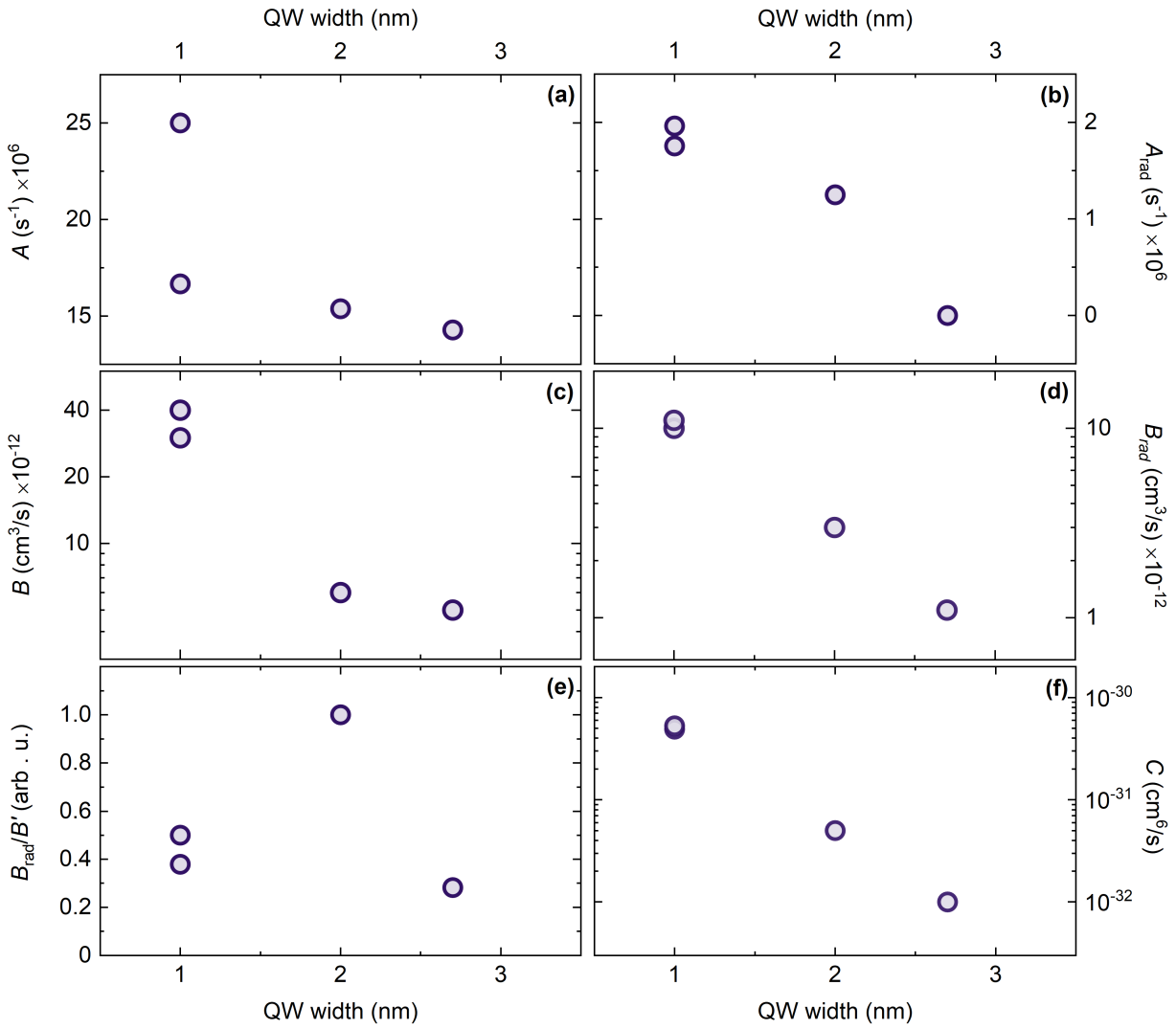

Figure S5. Dependences of recombination constants $A \approx A_{\mathrm{SRH}}$, A_{rad}, $B = B_{\mathrm{rad}} + B'$, B_{rad}, B_{rad}/B', and C against the QW width in the subset of samples with 25% indium content.

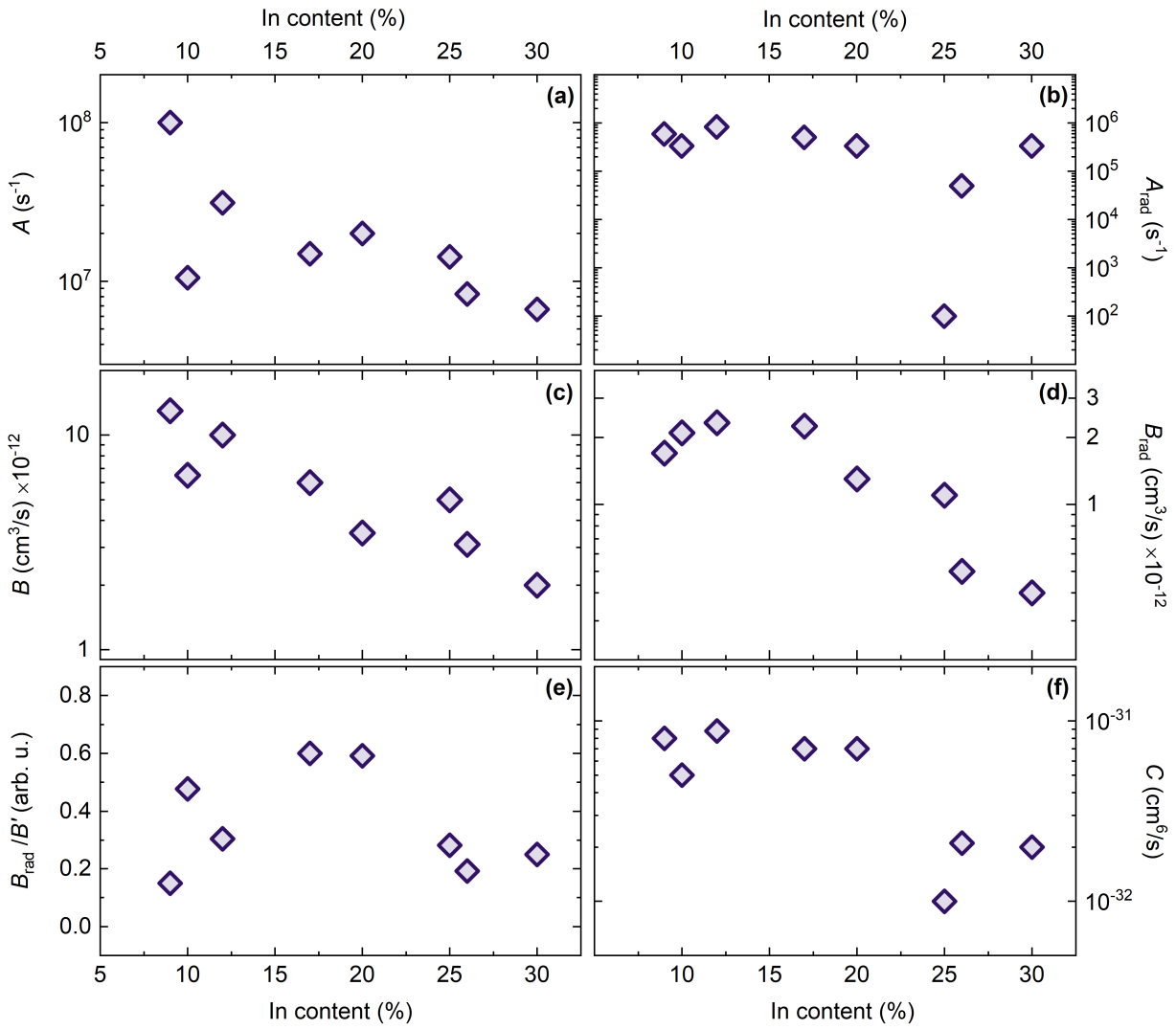

Figure S6. Dependences of recombination constants $A \approx A_{\mathrm{SRH}}$, A_{rad}, $B = B_{\mathrm{rad}} + B'$, B_{rad}, B_{rad}/B', and C against indium content in the subset of 3 nm thick QW samples.

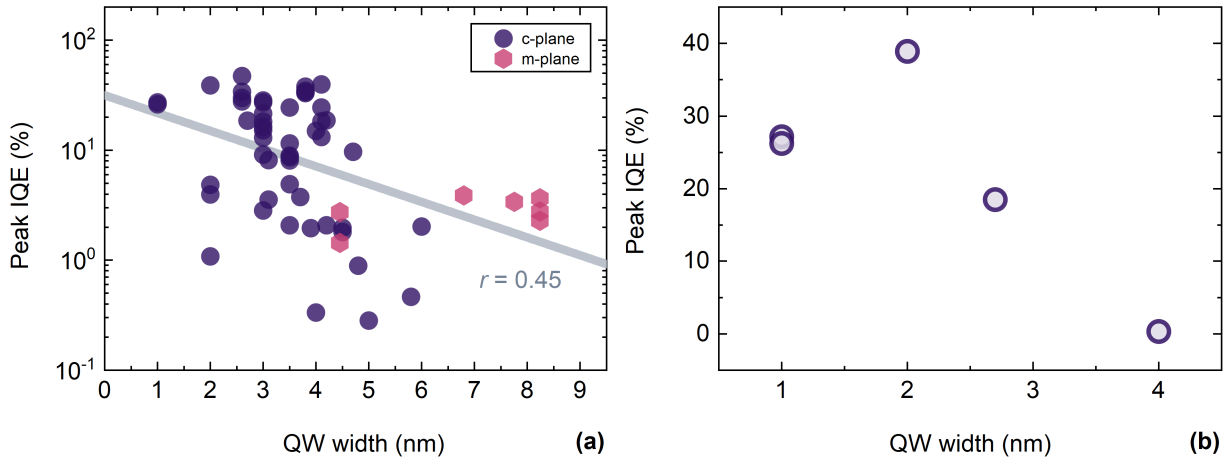

Figure S7. Dependence of peak IQE on the QW thickness in all samples (a) and in the subset of QW structures with 25% indium content (b). r stands for the Pearson's correlation coefficient, magenta hexagons indicate the nonpolar structures.